Journal of Oceanology and Limnology
Vol. 41 No. 1, P. 300-313, 2023
https://doi.org/10.1007/s00343-021-1307-3

Structural characterization of sulfated galactofucan from *Undaria pinnatifida* and its effect on type 2 diabetic mice*

Songze KE[1, #], Bo ZHANG[1, #], Yanlei YU[1, 4], Sijia WANG[1, 2], Weihua JIN[3], Jian WU[5], Jianwei CHEN[1, 4], Huawei ZHANG[1, 4], Bin WEI[1, 4, **], Hong WANG[1, 4, **]

[1] *College of Pharmaceutical Science & Collaborative Innovation Center of Yangtze River Delta Region Green Pharmaceuticals, Moganshan Research Institute at Deqing County Zhejiang University of Technology, Zhejiang University of Technology, Hangzhou 310014, China*

[2] *Center for Human Nutrition, David Geffen School of Medicine, University of California, Los Angeles CA 90024, USA*

[3] *College of Biotechnology and Bioengineering, Zhejiang University of Technology, Hangzhou 310014, China*

[4] *Key Laboratory of Marine Fishery Resources Exploitment & Utilization of Zhejiang Province, Hangzhou 310014, China*

[5] *Zhejiang Provincial Key Laboratory of Traditional Chinese Medicine Pharmaceutical Technology, Hangzhou 310014, China*

Received Sep. 19, 2021; accepted in principle Nov. 1, 2021; accepted for publication Dec. 27, 2021

Abstract A sulfated galactofucan designated as UpG was obtained from the brown algae *Undaria pinnatifida* by calcium chloride extraction. Chemical analyses showed that UpG is composed of galactose and fucose at a high sulfation level. Low-molecular weight UpGP-0.5 was prepared from UpG through acid hydrolysis for structure characterization. The backbones of UpG are determined to be α-(1,3)-Fuc, α-(1,4)-Gal, α-(1,3)-Gal, and α-(1,6)-Gal by GC-MS, FT-IR, NMR, and LC-MS analyses. Sulfate groups are modified at C2 and/or C4 of fucose and C3 and/or C4 of galactose. UpG could partially lower blood sugar and serum lipid levels in type 2 diabetic mice. Moreover, UpG treatment regulates the abundance of some specific gut microbiota, such as enriching the abundance of *Muribaculum* and Christensenellaceae, and reducing that of *Bilophila*, Tannerellaceae, *Candidatus Saccharimonas* and *Anaerotruncus*. The findings characterized the detailed structure of a sulfated galactofucan and investigated its potential for the treatment of type 2 diabetes mellitus.

Keyword: *Undaria pinnatifida*; galactofucan; structure; gut microbiota; diabetes

1 INTRODUCTION

Diabetes has been one of the three chronic diseases in the world. Type 2 diabetes mellitus, which accounted for more than 90% of diabetic patients, showing syndromes of decreasing insulin sensitivity or increased blood glucose and generally being associated with metabolic and genetic factors (DeFronzo et al., 2015; Marchetti, 2016). Metabolic disorder is a common feature of diabetic patients and is accompanied by the unbalance of carbohydrate, lipid metabolism, and gut microbiota, such as the variation of liver glycogen and serum lipid index (Sun et al., 2018a). Gut microbiota is a bioreactor that influences food metabolism and energy homeostasis in the body. The accumulating evidence indicated that the quantitative and qualitative discrepancies in intestinal flora appeared between type 2 diabetes and non-type 2 diabetes patients, and the specific diet intervention could be beneficial to modify the gut microbiota composition and alleviate type 2 diabetes, e.g., using polysaccharides (Diamant et al., 2011; Lin et al., 2019; Frost et al., 2021).

Undaria pinnatifida is a type of brown algae inhabiting the coastal areas of Asiatic and European countries, and it is a popular vegetable in these countries (Wang et al., 2018). In China, it is a Chinese herbal medicine, commonly used to treat nephropathy

* Supported by the National Key Research and Development Program (Nos. 2018YFC0311003, 2017YFE0103100), the National Natural Science Foundation of China (Nos. 81903534, 81773628, 81741165), and the High-Level Talent Special Support Plan of Zhejiang Province (No. 2019R52009)
** Corresponding authors: hongw@zjut.edu.cn; binwei@zjut.edu.cn
# Songze KE and Bo ZHANG contributed equally to this work and should be regarded as co-first authors.

and diuretic swelling. Polysaccharide is one of the active ingredients of *U. pinnatifida*, possessing diverse structure and activity, and the polysaccharide is usually identified as a sulphated galactofucan, mainly contains sulfate group, acetyl group, galactose, and fucose. Lee et al. (2004) and Hemmingson et al. (2006) reported that polysaccharides from *U. pinnatifida* has a complex skeleton (1→3-linked fucose, 1→3, 1→4, 1→6-linked galactose) and is sulfated at C2/C4 positions of fucose residues and C3/C6 positions of galactose residues. However, Koh et al. (2019) prepared a polysaccharide consisting of an alternating 1→3-linked fucose-galactose backbone with sulfation at C2/C4 position. Recent studies show that fucoidan possesses numerous bioactive properties such as antioxidant (Zhong et al., 2019), anticoagulant (Sun et al., 2018b), anti-cancer (Zhao et al., 2021), and anti-diabetes (Zhong et al., 2021) activities. Jiang et al. (2021) found that supplement *U. pinnatifida* could relieve high-fat diet-induced metabolic syndrome by reducing weight gain and fat accumulation, and maintained the homeostasis of microbiota. A previous work of ours shows that *U. pinnatifida* could significantly reduce the HFD/streptozocin-induced hyperglycemia (Zhong et al., 2021). However, the effect of polysaccharides from *U. pinnatifida* in regulating gut microbiota remains unclear.

In this study, a sulfated galactofucan was extracted from *U. pinnatifida*, separated in a weak anion exchange column, and subsequently hydrolyzed by diluted sulfuric acid to obtain a low-molecular weight galactofucan. The structure was determined by methylation analysis, MS, and NMR spectroscopy. The effect of the polysaccharide in streptozocin-induced diabetic mice was studied with physiological parameters and gut microbiota analyzed.

2 MATERIAL AND METHOD

2.1 Material

Undaria pinnatifida was collected in April 2019 in Rongcheng City, Shandong Province, China. Bio-Gel P-4 was obtained from Bio-Rad Pacific Ltd. (California, USA). Monosaccharide standards (fucose, mannose, glucose, galactose, rhamnose, and xylose) were provided by the Aladdin Chemistry Co., Ltd. (Shanghai, China). Sephacryl S-400 was purchased from GE Healthcare (USA). Streptozocin was obtained from Aladdin Chemistry Co., Ltd. (Shanghai, China).

2.2 Extraction and purification of polysaccharide

An amount of 100-g brown algae *U. pinnatifida* was added to 3 000-mL water containing 30-g calcium chloride, and extracted for 3 h at 100 ℃. The solution was cooled down to room temperature, centrifuged, and concentrated to 300 mL. The solution was dialyzed in pure water for 48 h, and then concentrated by rotary evaporator with a vacuum pump and precipitated by 75% ethanol. Crude polysaccharide was obtained using an infrared lamp.

The crude polysaccharide was fractionated by DEAE Sepharose Fast Flow column with water and different concentrations of NaCl, respectively. The 1.0–2.0-mol/L NaCl elution component (UpG) was collected and dialyzed by 14-kDa molecular weight cut-off membrane, precipitated by 75% ethanol and dried using an infrared lamp. The collected UpG (0.2 g) was redissolved in 1-mL water and further purified by Sephacryl S-400 (2.6 cm×100 cm) column with 0.5-mol/L ammonium bicarbonate as the elution solvent.

2.3 Hydrolysis and purification of *U. pinnatifida* polysaccharides

The homogeneous polysaccharide (UpG) was hydrolyzed by dilute sulfuric acid (pH=1) at 110 ℃ for 5 h. The hydrolysate was neutralized by barium hydroxide, centrifuged, concentrated, desalted on a Sephadex G-10 (3.8 cm×50 cm) column, and precipitated by 80% ethanol to obtain UpGP. The supernatant was concentrated, and further precipitation with 91% ethanol to obtain the sediment (UpG1). The UpGP was next purified by DEAE FF column with water and NaCl solution. 0.1–0.5-mol/L NaCl elution component was desalted by a 500-Da molecular weight cut-off membrane, concentrated, and lyophilized to obtain the low-molecular weight polysaccharide fraction (UpGP-0.5). And a Bio-Gel P-4 (1.0 cm×100 cm) column was used to separate UpG1 and elute with 0.5-mol/L ammonium bicarbonate. Oligosaccharides were collected and lyophilized.

2.4 Composition analysis

The total sugar was measured by phenol-sulfuric acid method (Lin and Pomeranz, 1968). The sulfate content was determined by barium chloride-gelatin method (Dodgson and Price, 1962). The monosaccharide composition was processed using pre-column derivatization and analyzed by HPLC system (Zhang et al., 2009). Briefly, a sample

(5 mg) was hydrolyzed in 4-mol/L trifluoroacetic acid (TFA) at 110 ℃ for 4 h. Then, the solution was dried in rotary evaporator with a vacuum pump. The monosaccharide mixture was reacted with 1-phenyl-3-methyl-5-pyrazolone (PMP) and detected by HPLC using Zorbax Eclipse XDB-C18 column (150 mm×4.6 mm, Agilent, USA). GPC-HPLC with TSK gel 5000 PWxl column and 3000 PWxl columns (7 μm, 7.8 mm×300 mm, TOSOH, Japan) in series were used to evaluate the molecular weight. 0.1-mol/L sodium nitrate was set as mobile phase at flow rate of 0.5 mL/min.

2.5 Deacetylation of polysaccharide

Deacetylation of *U. pinnatifida* polysaccharide was undertaken using the method reported by Chizhov et al. (1999). Briefly, polysaccharide (200 mg) dissolved in 6-mol/L ammonium hydroxide (20 mL) was kept overnight at 37 ℃. The reaction mixture was dialyzed by 14-kDa membrane, and concentrated and lyophilized to obtain deacetylated polysaccharide.

2.6 Desulfation of polysaccharides

The desulfated method of polysaccharide was undertaken as per Nagasawa et al. (1977) with minor modifications. The deacetylated polysaccharide was dissolved in water, and converted to acid form by a cation exchange column (1.0 cm×20 cm). The acidic components were collected, pH was adjusted to 9 with pyridine and lyophilized. The resulting polysaccharides were desulfated with a mixture solution (DMSO∶methanol∶pyridine=89∶10∶1), dialyzed by a 500-Da membrane, and concentrated and lyophilized to obtain sulfate-free polysaccharides.

2.7 Methylation analysis

The polysaccharide methylation was carried out as per Hakomori (1964). Briefly, 5-mg polysaccharide is mixed with NaH and anhydrous DMSO under N_2 protection, stirred for 4 h, and added 0.6-mL CH_3I to the reaction solution gradually, stirred for another 2 h, and 1-mL water was added to terminate the reaction. The methylated polysaccharides were extracted with CH_2Cl_2, and concentrated and lyophilized. The resulting polysaccharides were hydrolyzed by 2-mol/L TFA, reduced by $NaBD_4$ containing 0.05-mol/L NaOH acetylated by acetic anhydride, and finally analyzed on GC-MS devices.

2.8 The Fourier transform infrared spectrometer analysis

An amount of 1-mg polysaccharide was mixed with 99-mg KBr, pressed to a tablet, analyzed by a Fourier transform infrared spectrometer (Thermo Nicolet 6700, USA), and scanned at 400–4 000/cm.

2.9 MS analysis of oligosaccharide

Negative ESI-MS and MS^2 were carried out by AB SCIEX Triple TOF 5600^+ (USA). The sample of oligosaccharides are dissolved in 50% acetonitrile solution at a concentration of 0.1 mg/mL, and delivered by a syringe pump at flow rate of 5 μL/min.

2.10 Nuclear magnetic resonance spectroscopy

Polysaccharide (50 mg) was dissolved in D_2O (99.9%) followed by lyophilization for three times, and redissolved in 550-μL D_2O for NMR analysis. The 1D (^1H and ^{13}C) and 2D (HSQC, ^1H-^1H COSY, ^1H-^1H TOCSY, HMBC) spectrum were obtained by Bruker III 500 M (Bruker, Switzerland).

2.11 Animal experiment design

Five-week old C57BL/6J male mice, SPF grade, were obtained from Beijing Sipeifu Biotechnology Co., Ltd. (Beijing, China), randomly divided into 3 groups (n=5), adapted to a controlled environment with 12 h per light-dark cycle daily at 23±2 °C and fed with a normal diet (4% kcal fat, #MD 12033, Jiangsu Medicience Co., Ltd., Yangzhou, China). The control group (CON group, n=5) was fed with low-fat diet (LFD, 10% kcal fat and 71% kcal carbohydrate). The remaining mice were fed with high-fat diet (HFD, 60% kcal fat and 21% kcal carbohydrate) for six weeks. The diabetic model was successfully induced by intraperitoneal injection with streptozotocin (STZ) (40 mg/(kg·d)) for five days. The diabetic mice were separated into diabetic mice were not fed polysaccharide (MOD) group (n=5) and UpG group (n=5). The UpG group was orally administered with UpG at a dose of 200 mg/(kg·d) for nine weeks and fed with HFD at the same time. The MOD group fed with HFD only was set as the control. The fasting blood glucose was detected at tail vein using a glucometer in week 9 (fasting for 16 h). After 9 weeks, the mice were sacrificed. Cecal samples were collected, and stored at -80 ℃ for further use. The serum sample was obtained by centrifugation at 4 000 r/min, for 10 min at 4 ℃. The serum TG, TC, LDL-C, and HDL-C were evaluated using the reagent test kit purchased from

Nanjing Jiancheng Bioengineering Institute (Nanjing, China). All experiments were approved by the Ethics Committee of the Zhejiang University of Technology (2019081075).

2.12 Microbial community analysis

Each cecal sample in CON, MOD, and UpG groups was analyzed on Illumina Miseq platform. DNA extraction, amplification, purification, and sequencing were carried out in our previous study (Wei et al., 2020).

2.13 Bioinformatics analysis

Bioinformatics was analyzed as per our previous study (Wei et al., 2020) with a little modification. Briefly, the raw demultiplexed sequences were denoised and quality filtered using QIIME2. The remaining unique sequences were taxonomically classified using classify-sklearn against the SILVA 13_8 99% OTU reference sequences. Some feature tables about gut microbiota abundance and α-diversity indexes for further analysis.

2.14 Statistical analysis

Data are expressed in mean±SD. Two-tailed Student *t*-test and One-way ANOVA were performed to the discrepancy between the two groups ($P<0.05$) analyzed by software GraphPad (Ver.8.0).

3 RESULT AND DISCUSSION

3.1 Isolation and purification of UpG

The sulfated polysaccharide (UpG) was obtained from *U. pinnatifida* through calcium chloride extraction and weak anion exchange purification. The yield is 0.15%. The results of the chemical analysis are shown in Table 1. UpG contains a high level of sulfation groups (36.64%) and the total sugar is 48.73%. Monosaccharide analysis showed that UpG is consisted of galactose and fucose (the ratio of Gal∶Fuc=60∶40), known as galactofucan (Jin et al., 2020). The average molecular weight is approximately 453 kDa determined by GPC analysis using dextran as standard. UpG contains acetyl groups, which hindered the degree of methylation. Ammonium hydroxide is used to remove acetyl groups to obtain daUpG. The chemical characteristic of daUpG is similar to that of UpG. The low-molecular weight polysaccharide fraction UpGP-0.5 has the highest ratio of galactose (Gal∶Fuc≈10∶1) and lower molecular weight (3.2 kDa). The same observation was also made by Geng et al. (2018) in which glucofucogalactan is degraded by diluted acid, whose ratio of Gal∶Fuc (0.82∶1) was incresed to 1∶0.52. It is speculated that fucose is easier to fall off than galactose in hydrolysis process.

Table 1 The chemical characteristics of polysaccharides from *U. pinnatifida*

Sample	Total sugar (%)	Sulfate (%)	Uronic acid (%)	Molecular weight (kDa)	Monosaccharide	
					Gal (%)	Fuc (%)
UpG	48.73	36.64	5.85	453	59.69	40.31
UpG1	74.12	21.09	–	–	–	–
UpGP-0.5	52.94	27.69	9.86	3.20	91.85	8.15
daUpG	51.68	34.94	5.69	447	56.87	43.13

–: not detected. Gal: galactose; Fuc: fucose.

3.2 IR analysis

The IR spectrometry of UpG, daUpG, and UpGP-0.5 is shown in Fig.1. The strong and broad absorbance peaks at (3 417–3 443)/cm are accounted for the O-H stretching vibration (Choi et al., 2014). The band at approximately 2 940/cm is matched to C-H vibration in galactose and fucose (Deore and Mahajan, 2021). The band at (1 636–1 651)/cm is assigned to C=O vibration. The band at 1 400/cm is explained as C-H or C-O-H stretching vibration absorption (Chen et al., 2019). The band at (1 250–1 262)/cm is due to asymmetric S=O vibration. The peak around 1 055/cm indicate the presence of C-O-C and C-O-H (Raguraman et al., 2019). A shoulder peak at 1 732/cm in UpG (Fig.1a) indicates the presence of O-acetyl group. The distinct stretching peaks at 837.8 and 839/cm are mainly ascribed to the C-O-S bending vibration at C4. And the band at 826/cm suggested the presence of C3, but C4 sulfate substitution could not be excluded (Koh et al., 2019; Chen et al., 2020; Yang et al., 2021).

3.3 Methylation analysis

Methylation analysis of polysaccharide is a common method to decipher the structural characterizations of polysaccharides. To determine the position of sulfation and the type of glycosidic linkage, daUpG, UpGP-0.5, and their desulfated derivatives were methylated and determined on GC-MS at the same time. dsUpG (desulfated derivative of UpG) is composed of nine derivatives of partially methylated alditol acetates (PMAA), suggesting that the skeleton linkage of UpG is →3)Fuc(1→, →4)Gal(1→, →3)Gal(1→ and →6)

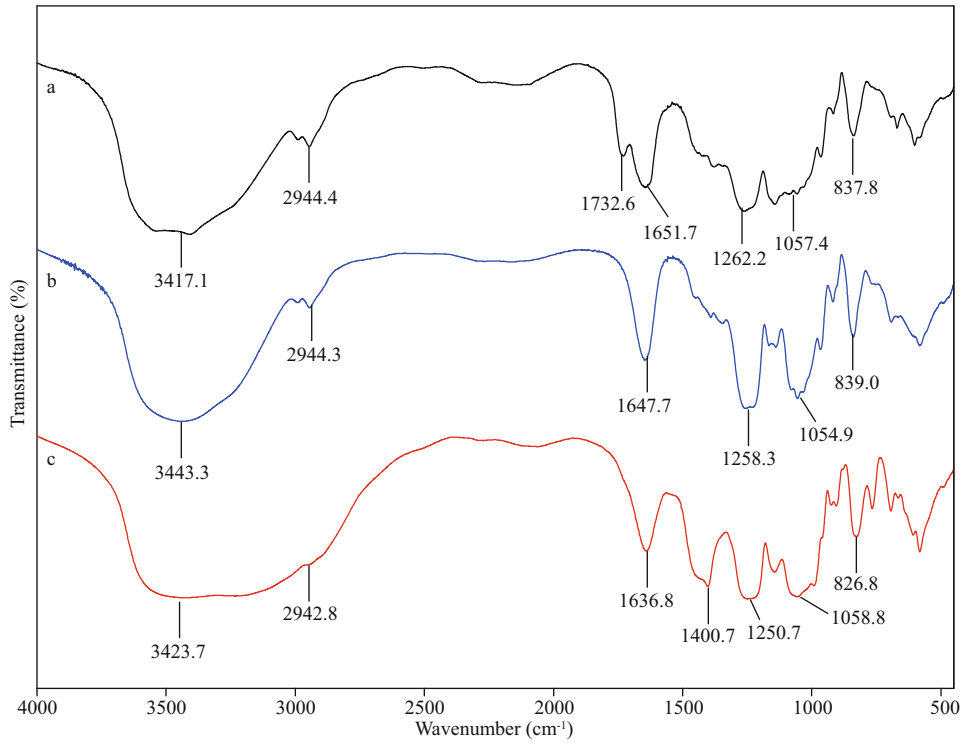

Fig.1 The IR spectrometry for UpG (a), daUpG (b), and UpGP-0.5 (c)

Table 2 Methylation analysis of fractions daUpG, UpGP-0.5, and their desulfated derivatives[#]

Position of O-methyl groups in	Deduced position of substitution	Peak area percentage (%)			
		daUpG	dsUpG*	UpGP-0.5	dsUpGP-0.5*
2,3,4-Fuc	Fuc(1→	0.78	2.82	–	0.57
2,4-Fuc	→3)Fuc(1→	4.26	17.16	2.35	3.48
2-Fuc	→3,4)Fuc(1→	16.19	10.21	1.46	–
4-Fuc	→2,3)Fuc(1→	4.93	–	1.01	–
Fuc	→2,3,4)Fuc(1→	17.34	–	–	–
Total Fuc		43.50	30.19	4.82	4.05
2,3,4,6-Gal	Gal(1→	1.10	19.32	2.19	18.16
2,3,6-Gal	→4)Gal(1→	2.27	12.07	5.49	17.29
2,4,6-Gal	→3)Gal(1→	11.74	18.52	24.21	22.19
2,3,4 -Gal	→6)Gal(1→	2.27	13.90	7.85	24.06
2,6-Gal	→3,4)Gal(1→	11.30	–	12.33	–
2,3-Gal	→4,6)Gal(1→	9.91	3.87	10.05	7.54
2,4-Gal	→3,6)Gal(1→	12.82	2.13	27.97	6.71
2-Gal	→3,4,6)Gal(1→	5.11	–	5.09	–
Total Gal		56.50	69.81	95.18	93.95

[#]: methylation analysis data for fractions daUpG and UpGP-0.5 (peak area percentage %); *: desulfated fraction. –: no data available.

Gal(1→ (in proportion of 17.16%, 12.07%, 18.52%, and 13.90%, respectively), and the main side chain is →3,4)Fuc(1→ (in proportion of 10.21%) (Table 2).

Compared with dsUpG, more types of glycosidic linkage are in daUpG (13 derivatives), which could provide location information of sulfate. The ratio of →3)Fuc(1→ increased from 4.26% to 17.16%, →3,4)Fuc(1→ and →2,3,4)Fuc(1→ dropped from 4.93% and 17.34% to 0 and 0%, respectively, indicating that the position of sulfation is occupied with C2/C4 of fucose. As shown in Table 2, the ratio of fucose in the methylation result of dsUpG decreased and galactosed

Table 3 The ^{1}H and ^{13}C chemical shifts of UpGP-0.5

	Residue	Chemical shift ($\times10^{-6}$)					
		H1/C1	H2/C2	H3/C3	H4/C4	H5/C5	H6/C6
A	→3)-α-L-Fuc-(1→	5.19/92.27	3.80/69.29	4.51/77.79	4.03/66.33	3.79/69.16	1.18/16.06
B	→3)-α-L-Fuc-(2SO_3^-)-(1→	5.24/99.97	3.77/82.40	4.54/77.59	3.40/71.44	3.74/70.60	1.12/16.03
C	→3)-α-L-Fuc-(4SO_3^-)-(1→	5.27/99.61	3.74/68.92	4.07/71.16	4.40/nd	3.88/68.86	1.18/16.06
D	β-D-Gal-(3SO_3^-)-(1→	4.55/96.05	3.76/69.28	4.16/78.43	3.72/68.62	4.00/68.11	3.65/60.41
E	→4)-α-D-Gal-(1→	5.21/100.10	3.73/69.00	4.03/66.54	3.62/74.64	3.87, 3.86/68.99	3.65/61.13
F	→3)-α-D-Gal-(1→	5.21/100.10	3.74/68.92	4.06/77.68	4.45/72.55	3.71/68.92	3.56/61.13
G	→6)-α-D-Gal-(3SO_3^-)-(1→	4.96/98.18	4.02/68.68	4.46/77.79	3.73/68.77	4.05/68.69	3.76/67.00
H	→4,6)-β-D-Gal-(1→	4.48/102.94	3.78/69.00	4.02/68.43	4.45/77.85	4.05/68.69	3.73/67.20
I	→6)-β-D-Gal-(3SO_3^-)-(1→	4.56/103.94	4.08/66.62	3.76/82.70	4.53/73.35	3.71/68.92	4.10/67.38
J	→6)-β-D-Gal-(4SO_3^-)-(1→	4.64/103.74	4.03/66.26	3.62/74.79	4.25/79.72	3.55/71.05	4.10/67.38
K	→3,6)-β-D-Gal-(1→	4.39/103.20	3.78/69.00	4.04/77.73	4.48/73.26	3.88/68.86	3.73/66.68

increased compared with daUpG. We speculate that the fucose is easier degraded than galactose in the course of desulfurization, resulting in the ratio of galactose increased and the difficulty to determine the location of sulfation and the linkage types of galactose in polysaccharide UpG (Wei et al., 2019). Therefore, these results can only be regarded as qualitative (Arata et al., 2015). The low-molecular weight polysaccharide fraction UpGP-0.5 and its desulfated derivative dsUpGP-0.5 were also methylated to study the structure features. For UpGP-0.5, the backbone chain is similar to daUpG. Compared UpGP-0.5 with dsUpGP-0.5, fucose is →3)Fuc(1→ (3.48%), and sulfated at C2/C4 of fucose. The ratio of →4)Gal(1→ increased by 11.80% and →3,4)Gal(1→ decreased by 12.33%, suggesting that the sulfation located at C3 of →4)Gal(1→. →6)Gal(1→ increased by 16.21%, →4,6)Gal(1→ and →3,6)Gal(1→ decreased by 2.51% and 21.26%, respectively, implying that the position of sulfate could be C3/C4 of →6)Gal(1→. The remaining linkages could contribute to Gal(1→, indicating that the side chain or sulfation located at C3/C4 of galactose. Therefore, (1→3)-linked fucose and (1→3), (1→4), (1→6)-linked galactose predominates in *U. pinnatifida* polysaccharides, and position 2 and 4 of fucose and 3 and 4 of galactose are occupied in sulfate. This finding is consistent with a previous report (Hemmingson et al., 2006).

3.4 NMR spectroscopy

The 1D (^{1}H and ^{13}C) and 2D (HSQC, ^{1}H-^{1}H COSY, HMBC, and ^{1}H-^{1}H TOCSY) NMR spectroscopy are used to estimate the structure of UpGP-0.5. 10 anomeric protons ((4.39–5.27)$\times10^{-6}$) and protons of methyl group of fucose (1.2×10^{-6}), are observed in the ^{1}H NMR spectrum of UpGP-0.5 (Fig.2a) (Wang et al., 2010). Meanwhile, the resonance signals of ^{13}C spectrum at 16×10^{-6} is also assigned to methyl group (Fig.2b) (Usoltseva et al., 2019). The intensive signals at (3.5–4.4)$\times10^{-6}$ in ^{1}H spectrum and (66–83)$\times10^{-6}$ in ^{13}C spectrum belong to C2–C5 of fucose and galactose (Li et al., 2015; Liu et al., 2021). All chemical shifts of UpGP-0.5 are shown in Table 3.

HSQC spectrum indicates that the anomeric regions of fucose are H_{A1}/C_{A1}-$5.19\times10^{-6}/92.27\times10^{-6}$, H_{B1}/C_{B1}-$5.24\times10^{-6}/99.97\times10^{-6}$, H_{C1}/C_{C1}-$5.27\times10^{-6}/99.61\times10^{-6}$, and the position 6 are H_{A6}/C_{A6} (H_{C6}/C_{C6})-$1.18\times10^{-6}/16.06\times10^{-6}$ and H_{B6}/C_{B6}-$1.12\times10^{-6}/16.03\times10^{-6}$, respectively (Fig.2c). According to ^{1}H-^{1}H COSY (Supplementary Fig.S1a), the former one is assigned to the structure →3)-α-L-Fuc-(1→, and the latter two are →3)-α-L-Fuc-(2SO_3^-)-(1→ and →3)-α-L-Fuc-(4SO_3^-)-(1→. The type of linkage in galactose is more complexity, of which contains three main linkage type: →4)-α-D-Gal-(1→, →3)-α-D-Gal-(1→ and →6)-α-D-Gal-(1→. So, referring to 2D spectrum (Fig.2c and Supplementary Fig.S1), the structure of low-molecular weight polysaccharide fraction UpGP-0.5 are shown in Fig.3.

3.5 Structural analysis of UpG1

UpG1 is composed of oligosaccharides, of which the total sugar and sulfated is 74.12% and 21.09%, respectively (Table 1). Then UpG1 was further separated using Bio-Gel P-4 column to obtain six fractions (U1, U2, U3, U4, U5, and U6). To determine the linkage between galactose and fucose, the negative ESI-MS was used to analyze these oligosaccharides

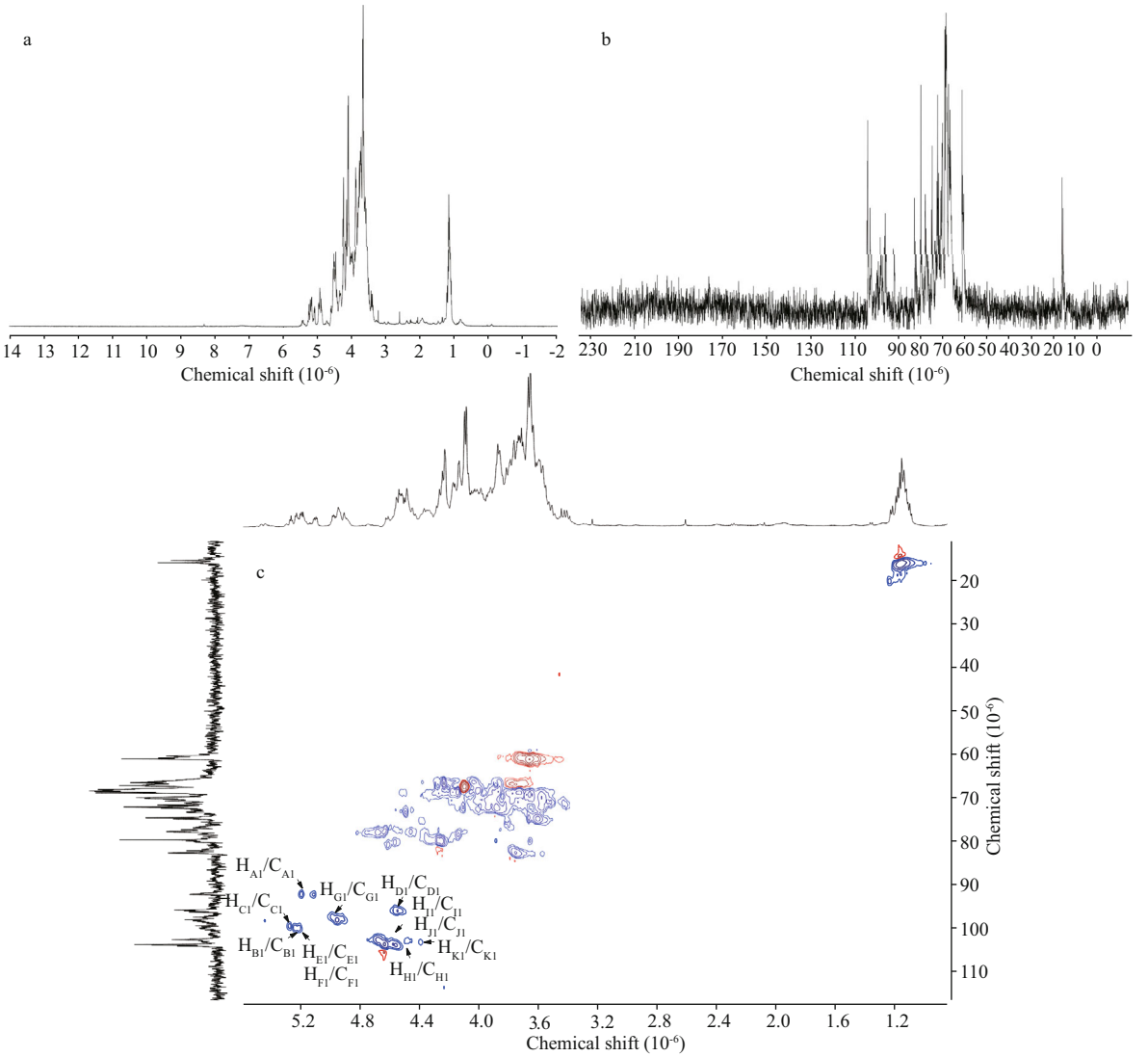

Fig.2 ^{1}H-NMR (a), ^{13}C-NMR (b), and HSQC (c) spectra of UpGP-0.5

(1) A H
···→3)-α-L-Fuc-(1→6)-β-D-Gal-(1→···
↑4

(2) I B
···→6)-α-D-Gal-(3SO_3^-)-(1→3)-α-L-Fuc-(2SO_3^-)-(1→···

(3) C H
···→3)-α-L-Fuc-(4SO3-)-(1→6)-β-D-Gal-(1→···
↑4

(4) D E
β-D-Gal-(3SO_3^-)-(1→4)-α-D-Gal-(1→···

(5) E I
···→4)-α-D-Gal-(1→6)-β-D-Gal-(3SO_3^-)-(1→···

(6) E J
···→4)-α-D-Gal-(1→6)-β-D-Gal-(4SO_3^-)-(1→···

(7) F K
···→3)-α-D-Gal-(1→6)-β-D-Gal-(1→···
↑3

(8) H G
···→6)-β-D-Gal-(1→6)-α-D-Gal-(3SO_3^-)-(1→···
↑4

(9) H E
···→6)-β-D-Gal-(1→4)-α-D-Gal-(1→···
↑4

(10) I K
···→6)-β-D-Gal-(3SO_3^--(1→6)-β-D-Gal-(1→···
↑3

(11) J G
···→6)-β-D-Gal-(4SO_3^-)-(1→6)-α-D-Gal-(3SO_3^-)-(1→···

(12) G E G E
···→6)-α-D-Gal-(3SO_3^-)-(1→4)-α-D-Gal-(1→6)-α-D-Gal-(3SO_3^-)-(1→4)-α-D-Gal-(1→···

Fig.3 Structural features of UpGP-0.5

components, which revealed a collection of poly-sulfated fucogalacto-oligosaccharide with DP: 2–5 (Table 4; Supplementary Fig.S2).

The oligosaccharide fraction U1 is mainly composed of three fragments *m*/*z* 301 (-3), 349.7 (-3) and 536 (-2), which is assigned to tri-sulfate

tetrasaccharide $[Gal_4(SO_3Na)_3\text{-}3Na]^{3-}$, tri-sulfate pentasaccharide $[Gal_4Fuc(SO_3Na)_3\text{-}3Na]^{3-}$ and $[Gal_4Fuc(SO_3Na)_3\text{-}2Na]^{2-}$. U2 also contains three ions, which is tri-sulfate trisaccharide $[Gal_2Fuc(SO_3Na)_3\text{-}3Na]^{3-}$ at *m/z* 241.67 (-3), di-sulfate trisaccharide $[Gal_2Fuc(SO_3Na)_2\text{-}2Na]^{2-}$ at *m/z* 323 (-2), and the sodium salt fragment $[Gal_2Fuc(SO_3Na)_3\text{-}2Na]^{2-}$ at *m/z* 374 (-2). The fragmentation ions for U3 at *m/z* 323 (-2), 331 (-2) and 567 (-1) are determined to $[Gal_2Fuc(SO_3Na)_2\text{-}2Na]^{2-}$, $[Gal_3(SO_3Na)_2\text{-}2Na]^{2-}$ and $[Gal_2FucSO_3Na\text{-}Na]^-$, respectively. For U4, U5, and U6, they are mainly composed of mono-sulfate oligosaccharides, which is *m/z* 567 (-1), 583 (-1), 421 (-1), 405 (-1), and 389 (-1). These results show that galactofucan UpG1 is a series of oligosaccharides consisted of alternately linked galactose and fucose, which is similar with a previous report (Vishchuk et al., 2013).

To further determine the characteristic of oligosaccharides, the ESI-MS/MS in negative ion mode was used to analyze the fragments of *m/z* 349.7 (-3), 323 (-2), 583 (-1), and 567 (-1).

The MS/MS of the tri-sulfate pentasaccharides $[Gal_4Fuc(SO_3Na)_3\text{-}3Na]^{3-}$ at *m/z* 349.7 (-3) show that the ion signals at *m/z* 138.97 and 183 arise from ring cleavage (Fig.4a). The monosulfate fucose at *m/z* 243 (Y_1) and monosulfate galactose at *m/z* 259 (Y_1) indicate that the sulfate located at fucose and galactose residue, and the three variants are $Gal(SO_3Na)Gal(SO_3Na)GalGalFuc(SO_3Na)$, $Gal(SO_3Na)GalGal(SO_3Na)GalFuc(SO_3Na)$, and $Gal(SO_3Na)GalGalGal(SO_3Na)Fuc(SO_3Na)$. Another highly intensive fragment ion B_4 at *m/z* 295 (-3) is known as $[Gal_4(SO_3Na)_3\text{-}3Na]^{3-}$, and there are no signals at *m/z* 218 and 262, suggesting the sulfate groups could not be simultaneous substitutions in galactose residue. Therefore, there are two isomers: $Gal(SO_3Na)Gal(SO_3Na)Gal(SO_3Na)GalFuc$ and $Gal(SO_3Na)Gal(SO_3Na)GalGal(SO_3Na)Fuc$. Thus, it is speculated that the ion at *m/z* 349.7 (-3) is composed of the five main isomers.

The negative tandem CID-MS^2 at *m/z* 323 (-2) suggested that the fragment ions at *m/z* 241 (B_1/Y_1), *m/z* 243 (Y_1), *m/z* 259 (Y_1), *m/z* 403 (B_2) and *m/z* 421 (Y_2) are derived from the breakage of glycosidic bonds (Fig.4b). According to the characteristic signal at *m/z* 403 (B_2), *m/z* 421 (Y_2), and *m/z* 243 (Y_1), the structural variant is $Gal(SO_3Na)GalFuc(SO_3Na)$. Due to the highest intensive fragment ion at *m/z* 241 (B_1/Y_1), anther isomer is $Gal(SO_3Na)FucGal(SO_3Na)$.

The ion at *m/z* 583 is assigned to $[Gal_3SO_3Na\text{-}Na]^-$ (Fig.4c). The X_2-type ions at *m/z* 463 and *m/z* 493 are the cross-ring cleavage, being derived from the reducing galactose. The major signal B_1 at *m/z* 241 is corresponded to dehydrated sulfate galactose, and the B_1 cleavage is easy to take place, because sulfate-containing B_1 is close to glycosidic bonds in structure (Anastyuk et al., 2012). Thus, the structure of *m/z* 583 is $Gal(SO_3Na)GalGal$.

Table 4 The negative ESI-MS of UpG1

Fraction	Ion	DP	*m/z*	Major structural composition
U1	301(-3)	4	903	$[Gal_4(SO_3Na)_3\text{-}3Na)]^{3-}$
	349.7 (-3)	5	1 049	$[Gal_4Fuc(SO_3Na)_3\text{-}3Na]^{3-}$
	536 (-2)	5	1 072	$[Gal_4Fuc(SO_3Na)_3\text{-}Na]^{2-}$
U2	241.67 (-3)	3	725	$[Gal_2Fuc(SO_3Na)_3\text{-}3Na]^{3-}$
	323 (-2)	3	646	$[Gal_2Fuc(SO_3Na)_2\text{-}2Na]^{2-}$
	374 (-2)	3	748	$[Gal_2Fuc(SO_3Na)_3\text{-}2Na]^{2-}$
U3	323(-2)	3	646	$[Gal_2Fuc(SO_3Na)_2\text{-}2Na]^{2-}$
	331(-2)	3	662	$[Gal_3(SO_3Na)_2\text{-}2Na]^{2-}$
	567(-1)	3	567	$[Gal_2FucSO_3Na\text{-}Na]^-$
U4	567 (-1)	3	567	$[Gal_2FucSO_3Na\text{-}Na]^-$
	583 (-1)	3	583	$[Gal_3SO_3Na\text{-}Na]^-$
U5	389 (-1)	2	389	$[Fuc_2SO_3Na\text{-}Na]^-$
	421 (-1)	2	421	$[Gal_2SO_3Na\text{-}Na]^-$
	567(-1)	3	567	$[Gal_2FucSO_3Na\text{-}Na]^-$
	583 (-1)	3	583	$[Gal_3SO_3Na\text{-}Na]^-$
U6	405 (-1)	2	405	$[GalFucSO_3Na\text{-}Na]^-$
	421 (-1)	2	421	$[Gal_2SO_3Na\text{-}Na]^-$

The MS^2 of ion at *m/z* 567 is mono-sulfate galactofucooligosaccharides (Fig.4d). Two low intensive peaks at *m/z* 243 (Y_1) and 405 (Y_1) indicate that the structure is $GalGalFuc(SO_3Na)$. The characteristic ion peaks at *m/z* 241 and 421 are assigned to sulfate at galactose, suggesting that the isomer is $FucGalGal(SO_3Na)$. According to these signals at *m/z* 259 and *m/z* 405, the trace isomer could be $GalFucGal(SO_3Na)$. Therefore, the oligosaccharide $[Gal_2FucSO_3Na\text{-}Na]^-$ has three variants: $GalGalFuc(SO_3Na)$, $FucGalGal(SO_3Na)$, and $GalFucGal(SO_3Na)$.

The NMR spectra of UpGP-0.5, methylation analysis, and ESI-MS/MS reveal the structural characteristics of UpG. UpG is a complex branched polysaccharide, and composed of alternative connected galactose and fucose. The structural backbone of UpG is α-(1,3)-Fuc, α-(1,3)-Gal, α-(1,4)-Gal, and α-(1,6)-Gal, and the sulfate group are occupied by fucose (C2 and/or C4) and galactose (C3 and/or C4). Previous studies reported that the

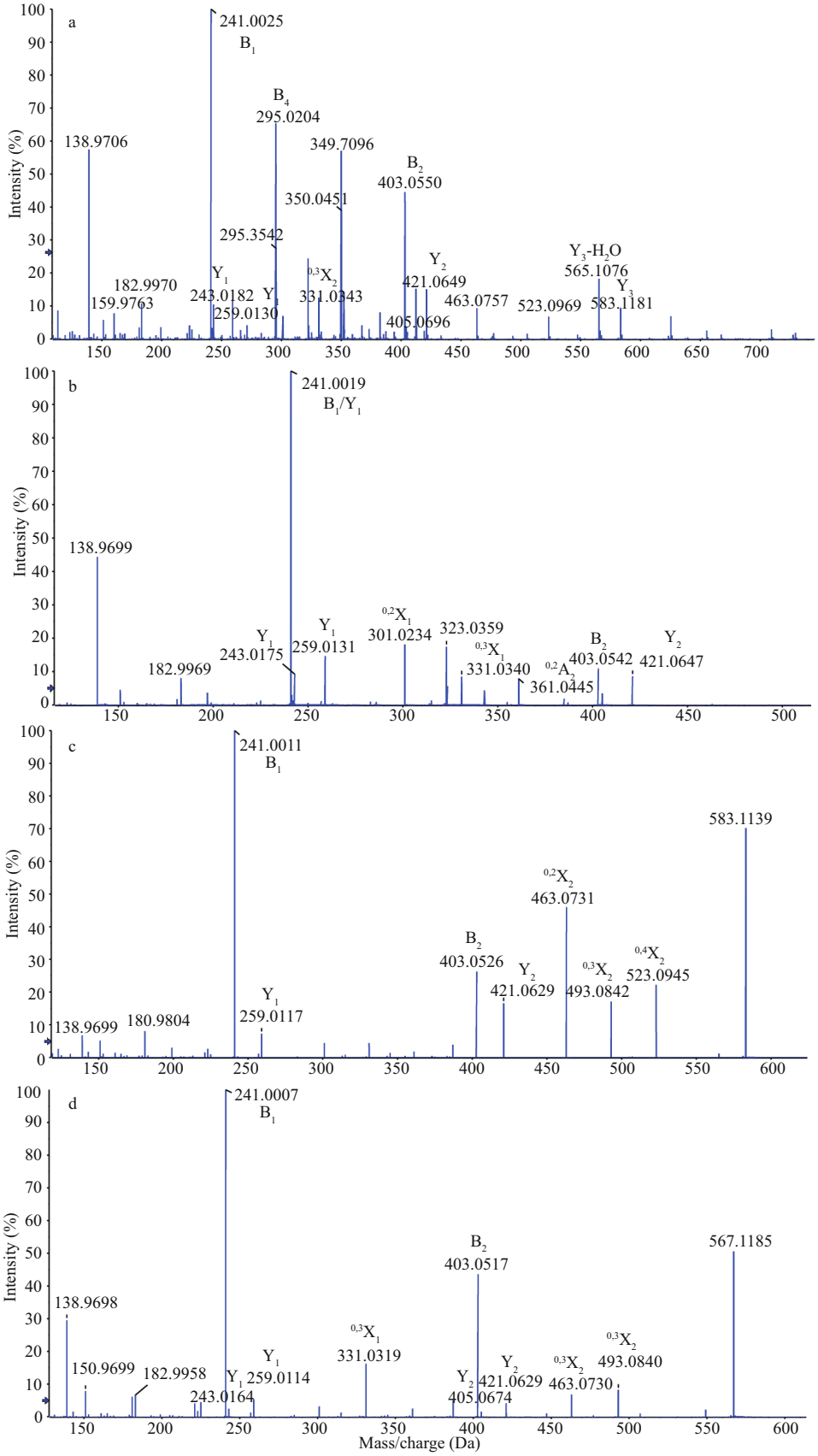

Fig.4 Negative-ion mode ESI-MS/MS spectra of the ions at *m*/*z* 349.7 (-3) (a), 323 (-2) (b), 583 (-1) (c), and 567 (-1) (d)

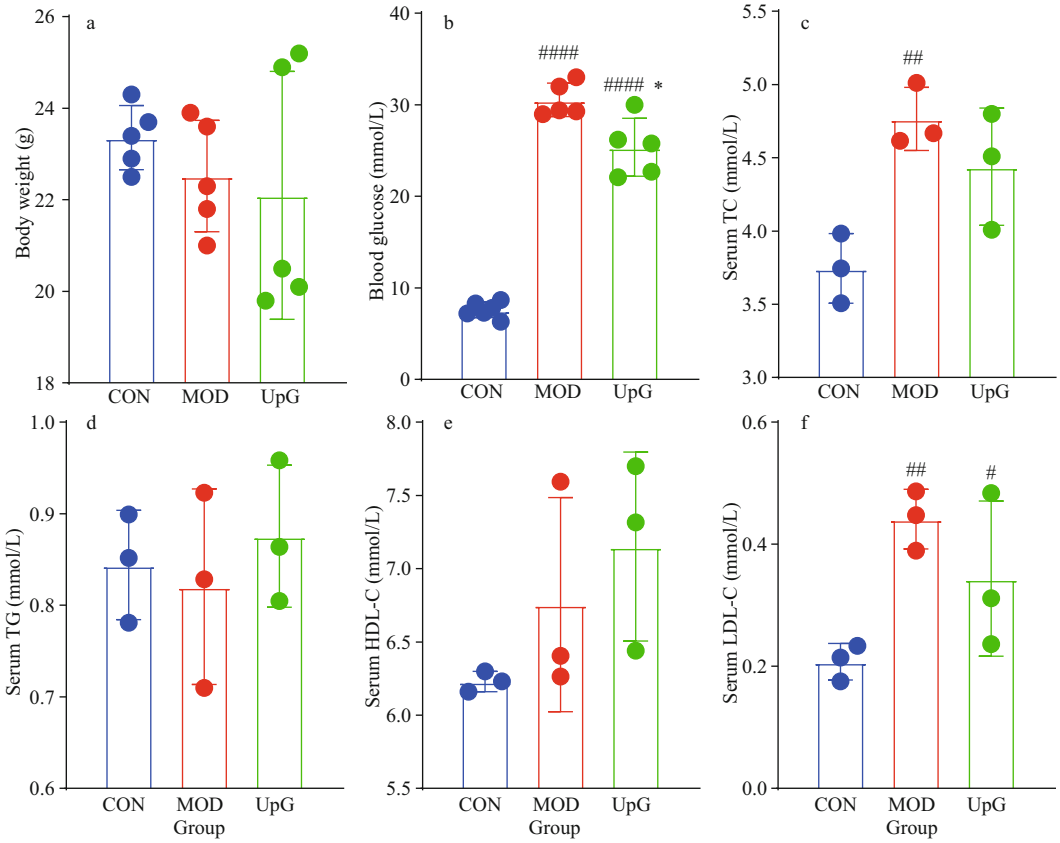

Fig.5 The effect of UpG on body weight in week 9 (a), fasting blood glucose (b), serum TC (c), TG (d), HDL-C (e), and LDL-C (f)

Values are mean±SD (n=3–5). #: P<0.05: ##: P<0.01; ####: P<0.000 1 vs. CON. *: P<0.05 vs. MOD.

skeleton of polysaccharides from *U. pinnatifida* was an alternating 1→3 fucose and 1→3 galactose (Hemmingson et al., 2006; Koh et al., 2019). Lee et al. (2018) found that galactofucan from *U. pinnatifida* has a complex structure with various linkages (1→3 fucose, 1→3 and 1→6 galactose), and sulphate is substituted at 2- or 4-positions of fucose, and at 3 positions of galactose. These findings highlight the structural diversity of *U. pinnatifida* polysaccharides.

3.6 Effect of UpG on the physiological indexes of diabetic mice

C57BL/6J male mice was treated by HFD and STZ to induce diabetes, and the effect of UpG was investigated on the diabetic model. After 9 weeks, MOD mice (fed with a HFD) with no UpG supplement exhibited severe symptoms of diabetes, including higher blood-glucose level, serum TC and LDL-C compared with the CON group (fed with a LFD) (Fig.5b–c, f). There was no significant difference in body weight among the three groups (CON, MOD, and UpG) in week 9 (Fig.5a). Interestingly, administration of UpG could partially decrease the fasting blood-glucose level (Fig.5b). The average levels of serum TC and LDL-C in the UpG group are 6.8% and 22.1% lower than those of the MOD group (Fig.5c & f). However, there are no significant difference among CON, MOD, and UpG groups in serum TG and HDL-C (Fig.5d–e). These results indicate that UpG could partially lower blood sugar and serum lipid levels in type 2 diabetic mice. Polysaccharides from *U. pinnatifida* with anti-diabetes effect were reported by Jia et al. (2020) and Zhong et al. (2021) found that polysaccharide from *U. pinnatifida* composed of fucose, mannose, galactose, and glucuronic acid (the ratio was 33.33%, 17.55%, 23.72%, and 9.68%, respectively) could significantly alleviate diabetes by reducing fasting blood-glucose level, serum TC, and TG. In addition, Zhong et al. (2021) showed that Up-U consisted of mannose, rhamnose, glucuronic acid, glucose, galactose, xylose, and fucose could remarkably decrease the blood-glucose level in vivo or in vitro. In the present study, UpG composed of galactose and fucose (the ratio is 60∶40) could only slightly reverse hyperlipemia and hyperglycemia induced by

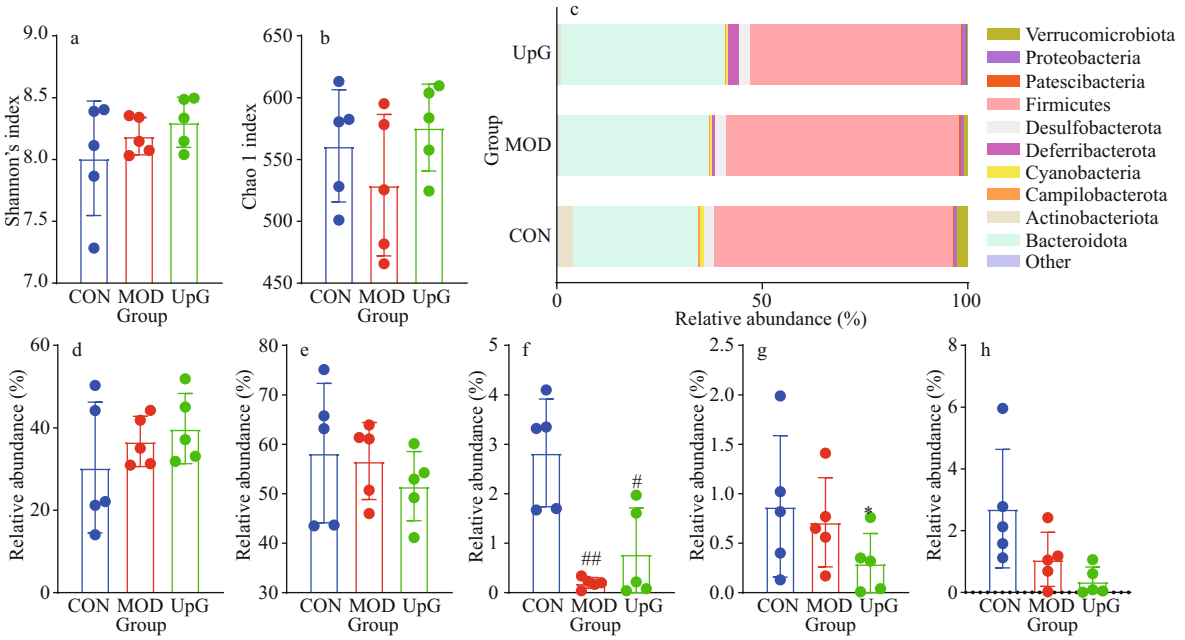

Fig.6 The effect of polysaccharide in regulating fecal microbiota

a. Shannon index; b. Chao 1 index; c. the heatmap of phylum; d. the abundance of Bacteroidetes; e. Firmicutes; f. Actinobacteria g. Cyanobacteria; h. Verrucomicrobia. Values are mean±SD (n=5). #: P<0.05; ##: P<0.01 vs. CON. *: P<0.05 vs. MOD.

diabetes. It is concluded that the anti-diabetic effect of *Undaria pinnatifida* polysaccharides is closely associated with their chemical structures.

3.7 Effect of UpG in regulating gut microbiota

To investigate the effect of polysaccharide UpG on diabetic mice in regulating gut microbiota, the 16S rRNA was employed to analyze the cecal contents. According to Shannon and Chao1 index in the three groups (CON, MOD and UpG) (Fig.6a–b), there are no significant difference among these groups on the species diversity and richness. The abundance of gut microbiota composition at phylum level is shown in Fig.6c. The number of Actinobacteria significantly decreased in MOD group (Fig.6f), which is a common phenomenon and has been reported previously (Wang et al., 2019). However, the abundance of Bacteroidetes, Firmicutes, and Cyanobacteria in MOD group show no significant difference comparing with CON group (Fig.6–e, g). The finding indicates that high carbohydrate in the LFD can also cause gut microbiota dysbiosis. Polysaccharide UpG treatment could increase the number of Actinobacteria (Fig.6f). Cyanobacteria, a bacterium related to colitis (Wang et al., 2020), could be significantly reduced by UpG (Fig.6g). For Verrucomicrobia, UpG could not reverse the decrease induced by diabetes compared with MOD group (Fig.6h).

Furthermore, we studied the gut microbiota community at the genus level. The most significant abundance bacteria (*Muribaculum*, Christensenellaceae, *Bilophila*, Tannerellaceae, *Candidatus Saccharimonas*, and *Anaerotruncus*) with special changes are further analyzed (Fig.7). Compared with CON group, the abundance of *Muribaculum* and Christensenellaceae decrease, while abundance of *Bilophila*, Tannerellaceae, *Candidatus Saccharimonas*, and *Anaerotruncus* increase in MOD group. Under diabetic model, the administration of polysaccharide UpG could enrich *Muribaculum* (Fig.7b), whose number is negatively correlated with the extent of obesity and inflammation (Li et al., 2020; Song et al., 2021). And UpG also increase the number of Christensenellaceae (Fig.7c). As shown in Fig.7d, UpG treatment could reduce the number of *Bilophila*. *Bilophila wadsworthia* is reported to be associated with metabolic syndrome and inflammation, and show negative effects on hepatic function, glucose, and lipid metabolism in HFD-treated mice (Natividad et al., 2018), suggesting that the anti-diabetic effect of UpG may be associated with the regulation of *Bilophila*. UpG supplementation significantly counteract the increase of *Anaerotruncus* (P<0.05, UpG vs. MOD), Tannerellaceae (P<0.01, UpG vs. MOD), and *Candidatus Saccharimonas* (P<0.05, UpG vs. MOD) in type 2 diabetic mice (Fig.7e–h). Generally, it is implied that UpG could alleviate diabetes symptoms via maintaining gut microbiota balance.

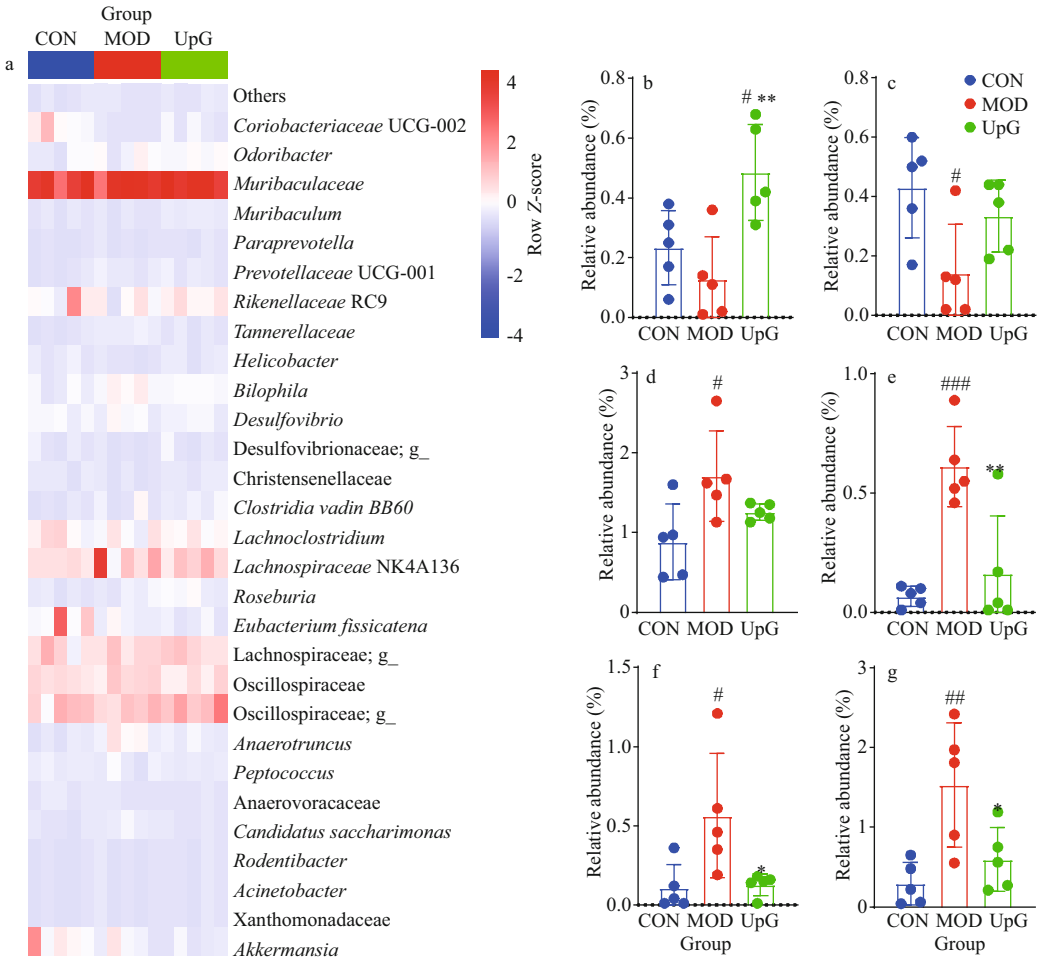

Fig.7 The effect of polysaccharide in regulating fecal microbiota in genus level

a. the heatmap; b. the abundance of *Muribaculum*; c. Christensenellaceae; d. *Bilophila*; e. Tannerellaceae; f. *Candidatus Saccharimonas*; g. *Anaerotruncus*. Values are mean±SD (n=5). #: P<0.05; ##: P<0.01; ###: P<0.001, vs. CON. *: P<0.05; **: P<0.01, vs. MOD.

4 CONCLUSION

A sulfated galactofucan, UpG, was obtained from *U. pinnatifida* by calcium chloride extraction. The monosaccharide analysis implied that UpG is composed of mainly fucose and galactose. Its backbone is consisted of α-(1,3)-Fuc, α-(1,4)-Gal, α-(1,3)-Gal, and α-(1,6)-Gal with high degree of branching, and position 2 and/or 4 of fucose and 3 and/or 4 of galactose are occupied by sulfate. In diabetic mice model, UpG could modulate physiological disorders by decreasing the level of blood glucose and LDL-C, and promote the abundance of *Muribaculum* and Christensenellaceae, and reduce *Bilophila*, Tannerellaceae, *Candidatus Saccharimonas* and *Anaerotruncus*. Therefore, the galactofucan UpG from *U. pinnatifida* is characterized as a highly branched polysaccharide and the galactofucan showed some potential for the treatment of type 2 diabetes mellitus.

5 SUPPORTING INFORMATION

The 2D spectra ^{1}H-^{1}H COSY, ^{1}H-^{1}H TOCSY and HMBC of UpGP-0.5 (Supplementary Fig. S1). Negative-ion mode ESI- MS spectra of the oligosaccharide fractions U1, U2, U3, U4, U5 and U6 (Supplementary Fig.S2).

6 DATA AVAILABILITY STATEMENT

The data that support the finding of this study are available from the corresponding author.

7 AUTHOR CONTRIBUTION

Songze KE and Bo ZHANG analyzed the data and drafted the manuscript. Yanlei YU and Sijia WANG helped with the biological experiments. Weihua JIN and Huawei ZHANG provided valuable intellectual input. Jianwei CHEN and Jian WU provided polysaccharide sample. Hong WANG and Bin WEI designed the experiment and revised the manuscript.

References

Anastyuk S D, Imbs T I, Shevchenko N M et al. 2012. ESIMS analysis of fucoidan preparations from *Costaria costata*, extracted from alga at different life-stages. *Carbohydrate Polymers*, **90**(2): 993-1002.

Arata P X, Quintana I, Canelón D J et al. 2015. Chemical structure and anticoagulant activity of highly pyruvylated sulfated galactans from tropical green seaweeds of the order Bryopsidales. *Carbohydrate Polymers*, **122**: 376-386.

Chen P L, Lei S Z, Chen Y Y et al. 2020. Structural characterization of a novel galactoglucan from *Fortunella margarita* and its molecular structural change following simulated digestion *in vitro*. *Journal of Functional Foods*, **71**: 104024.

Chen X Y, Ji H Y, Xu X M et al. 2019. Optimization of polysaccharide extraction process from *Grifola frondosa* and its antioxidant and anti-tumor research. *Journal of Food Measurement and Characterization*, **13**(1): 144-153.

Chizhov A O, Dell A, Morris H R et al. 1999. A study of fucoidan from the brown seaweed *Chorda filum*. *Carbohydrate Research*, **320**(1-2): 108-119.

Choi J I, Lee S G, Han S J et al. 2014. Effect of gamma irradiation on the structure of fucoidan. *Radiation Physics and Chemistry*, **100**: 54-58.

DeFronzo R A, Ferrannini E, Groop L et al. 2015. Type 2 diabetes mellitus. *Nature Reviews Disease Primers*, **1**(1): 15019.

Deore U V, Mahajan H S. 2021. Isolation and structural characterization of mucilaginous polysaccharides obtained from the seeds of *Cassia uniflora* for industrial application. *Food Chemistry*, **351**: 129262.

Diamant M, Blaak E E, de Vos W M. 2011. Do nutrient-gut-microbiota interactions play a role in human obesity, insulin resistance and type 2 diabetes? *Obesity Reviews*, **12**(4): 272-281.

Dodgson K S, Price R G. 1962. A note on the determination of the ester sulphate content of sulphated polysaccharides. *Biochemical Journal*, **84**(1): 106-110.

Frost F, Kacprowski T, Rühlemann M et al. 2021. Long-term instability of the intestinal microbiome is associated with metabolic liver disease, low microbiota diversity, diabetes mellitus and impaired exocrine pancreatic function. *Gut*, **70**(3): 522-530.

Geng L H, Zhang Q B, Wang J et al. 2018. Glucofucogalactan, a heterogeneous low-sulfated polysaccharide from *Saccharina japonica* and its bioactivity. *International Journal of Biological Macromolecules*, **113**: 90-97.

Hakomori S I. 1964. A rapid permethylation of glycolipid, and polysaccharide catalyzed by methylsulfinyl carbanion in dimethyl sulfoxide. *The Journal of Biochemistry*, **55**(2): 205-208.

Hemmingson J A, Falshaw R, Furneaux R H et al. 2006. Structure and antiviral activity of the galactofucan sulfates extracted from *Undaria pinnatifida* (Phaeophyta). *Journal of Applied Phycology*, **18**(2): 185-193.

Jia R B, Wu J, Li Z R et al. 2020. Comparison of physicochemical properties and antidiabetic effects of polysaccharides extracted from three seaweed species. *International Journal of Biological Macromolecules*, **149**: 81-92.

Jiang P R, Zheng W Y, Sun X N et al. 2021. Sulfated polysaccharides from *Undaria pinnatifida* improved high fat diet-induced metabolic syndrome, gut microbiota dysbiosis and inflammation in BALB/c mice. *International Journal of Biological Macromolecules*, **167**: 1587-1597.

Jin W H, Jiang D, Zhang W J et al. 2020. Interactions of fibroblast growth factors with sulfated galactofucan from *Saccharina japonica*. *International Journal of Biological Macromolecules*, **160**: 26-34.

Koh H S A, Lu J, Zhou W B. 2019. Structure characterization and antioxidant activity of fucoidan isolated from *Undaria pinnatifida* grown in New Zealand. *Carbohydrate Polymers*, **212**: 178-185.

Lee J B, Hayashi K, Hashimoto M et al. 2004. Novel antiviral fucoidan from sporophyll of *Undaria pinnatifida* (Mekabu). *Chemical and Pharmaceutical Bulletin*, **52**(9): 1091-1094.

Lee J, Lee S, Synytsya A et al. 2018. Low molecular weight mannogalactofucans derived from *Undaria pinnatifida* induce apoptotic death of human prostate cancer cells in vitro and in vivo. *Marine Biotechnology*, **20**(6): 813-828.

Li L L, Wang Y T, Zhu L M et al. 2020. Inulin with different degrees of polymerization protects against diet-induced endotoxemia and inflammation in association with gut microbiota regulation in mice. *Scientific Reports*, **10**(1): 978.

Li N, Mao W J, Yan M X et al. 2015. Structural characterization and anticoagulant activity of a sulfated polysaccharide from the green alga *Codium divaricatum*. *Carbohydrate Polymers*, **121**: 175-182.

Lin F D, Yang D D, Huang Y Y et al. 2019. The potential of neoagaro-oligosaccharides as a treatment of type II diabetes in mice. *Marine Drugs*, **17**(10): 541.

Lin F M, Pomeranz Y. 1968. Effect of borate on colorimetric determinations of carbohydrates by the phenol-sulfuric acid method. *Analytical Biochemistry*, **24**(1): 128-131.

Liu X, Xi X Y, Jia A R et al. 2021. A fucoidan from *Sargassum fusiforme* with novel structure and its regulatory effects on intestinal microbiota in high-fat diet-fed mice. *Food Chemistry*, **358**: 129908.

Marchetti P. 2016. Islet inflammation in type 2 diabetes. *Diabetologia*, **59**(4): 668-672.

Nagasawa K, Inoue Y, Kamata T. 1977. Solvolytic desulfation of glycosaminoglycuronan sulfates with dimethyl sulfoxide containing water or methanol. *Carbohydrate Research*, **58**(1): 47-55.

Natividad J M, Lamas B, Pham H P et al. 2018. *Bilophila wadsworthia* aggravates high fat diet induced metabolic dysfunctions in mice. *Nature Communications*, **9**(1): 2802.

Raguraman V, L S A, J J et al. 2019. Sulfated polysaccharide from *Sargassum tenerrimum* attenuates oxidative stress

induced reactive oxygen species production in *in vitro* and in zebrafish model. *Carbohydrate Polymers*, **203**: 441-449.

Song Y J, Shen H T, Liu T T et al. 2021. Effects of three different mannans on obesity and gut microbiota in high-fat diet-fed C57BL/6J mice. *Food & Function*, **12**(10): 4606-4620.

Sun W L, Zhang B W, Yu X X et al. 2018a. Oroxin A from *Oroxylum indicum* prevents the progression from prediabetes to diabetes in streptozotocin and high-fat diet induced mice. *Phytomedicine*, **38**: 24-34.

Sun Y H, Chen X L, Liu S et al. 2018b. Preparation of low molecular weight *Sargassum fusiforme* polysaccharide and its anticoagulant activity. *Journal of Oceanology and Limnology*, **36**(3): 882-891.

Usoltseva R V, Anastyuk S D, Surits V V et al. 2019. Comparison of structure and *in vitro* anticancer activity of native and modified fucoidans from *Sargassum feldmannii* and *S. duplicatum*. *International Journal of Biological Macromolecules*, **124**: 220-228.

Vishchuk O S, Ermakova S P, Zvyagintseva T N. 2013. The fucoidans from brown algae of Far-Eastern seas: anti-tumor activity and structure-function relationship. *Food Chemistry*, **141**(2): 1211-1217.

Wang H Y, Guo L X, Hu W H et al. 2019. Polysaccharide from tuberous roots of *Ophiopogon japonicus* regulates gut microbiota and its metabolites during alleviation of high-fat diet-induced type-2 diabetes in mice. *Journal of Functional Foods*, **63**: 103593.

Wang J J, Zhu G N, Sun C et al. 2020. TAK-242 ameliorates DSS-induced colitis by regulating the gut microbiota and the JAK2/STAT3 signaling pathway. *Microbial Cell Factories*, **19**(1): 158.

Wang J, Zhang Q B, Zhang Z S et al. 2010. Structural studies on a novel fucogalactan sulfate extracted from the brown seaweed *Laminaria japonica*. *International Journal of Biological Macromolecules*, **47**(2): 126-131.

Wang L, Park Y J, Jeon Y J et al. 2018. Bioactivities of the edible brown seaweed, *Undaria pinnatifida*: a review. *Aquaculture*, **495**: 873-880.

Wei B, Zhong Q W, Ke S Z et al. 2020. *Sargassum fusiforme* polysaccharides prevent high-fat diet-induced early fasting hypoglycemia and regulate the gut microbiota composition. *Marine Drugs*, **18**(9): 444.

Wei X Q, Cai L Q, Liu H L et al. 2019. Chain conformation and biological activities of hyperbranched fucoidan derived from brown algae and its desulfated derivative. *Carbohydrate Polymers*, **208**: 86-96.

Yang Y J, Hu T, Li J J et al. 2021. Structural characterization and effect on leukopenia of fucoidan from *Durvillaea antarctica*. *Carbohydrate Polymers*, **256**: 117529.

Zhang J J, Zhang Q B, Wang J et al. 2009. Analysis of the monosaccharide composition of fucoidan by precolumn derivation HPLC. *Chinese Journal of Oceanology and Limnology*, **27**(3): 578-582.

Zhao Y, Feng Y Y, Jing X et al. 2021. Structural characterization of an alkali-soluble polysaccharide from *Angelica sinensis* and its antitumor activity *in vivo*. *Chemistry & Biodiversity*, **18**(6): e2100089.

Zhong Q W, Wei B, Wang S J et al. 2019. The antioxidant activity of polysaccharides derived from marine organisms: an overview. *Marine Drugs*, **17**(12): 674.

Zhong Q W, Zhou T S, Qiu W H et al. 2021. Characterization and hypoglycemic effects of sulfated polysaccharides derived from brown seaweed *Undaria pinnatifida*. *Food Chemistry*, **341**: 128148.

Electronic supplementary material

Supplementary material (Supplementary Figs.S1–S2) is available in the online version of this article at https://doi.org/10.1007/s00343-021-1307-3.